

Origin of magnetic moments and presence of a resonating valence bond state in Ba_2YIrO_6

Abhishek Nag,¹ Sayantika Bhowal,² M. M. Sala,³ A. Efimenko,³
F. Bert,⁴ P. K. Biswas,⁵ A. D. Hillier,⁵ M. Itoh,⁶ S. D. Kaushik,⁷
V. Siruguri,⁷ C. Meneghini,⁸ I. Dasgupta,^{2,9} and Sugata Ray^{1,9,*}

¹*Department of Materials Science, Indian Association for
the Cultivation of Science, Jadavpur, Kolkata 700032, India*

²*Department of Solid State Physics,
Indian Association for the Cultivation of Science, Jadavpur, Kolkata 700032, India*

³*ESRF-The European Synchrotron, 71 Avenue des Martyrs, 38000 Grenoble, France*

⁴*Laboratoire de Physique des Solides, CNRS, Univ. Paris-Sud,
Université Paris-Saclay, 91405 Orsay Cedex, France*

⁵*ISIS Facility, Rutherford Appleton Laboratory,
Chilton, Didcot, Oxon OX110QX, United Kingdom*

⁶*Materials and Structures Laboratory, Tokyo Institute of Technology,
4259 Nagatsuta, Yokohama 226-8503, Japan*

⁷*UGC-DAE Consortium for Scientific Research Mumbai Centre,
Bhabha Atomic Research Centre, Mumbai, 400085, India*

⁸*Dipartimento di Scienze, Università Roma Tre,
Via della Vasca Navale, 84 I-00146 Roma, Italy*

⁹*Centre for Advanced Materials, Indian Association for the
Cultivation of Science, Jadavpur, Kolkata 700032, India*

Abstract

While it was speculated that $5d^4$ systems would possess non-magnetic $J = 0$ ground state due to the presence of strong spin-orbit coupling, this state has remained elusive to experimentalists till now. A puzzling case is that of Ba_2YIrO_6 , which in spite of having a perfectly cubic structure with largely separated Ir^{5+} ions has shown presence of magnetic moments in several recent reports. Theoretical calculations by two groups however, contradict each other on the presence of magnetic moments in this system. In this paper we show from Resonant Inelastic X-ray Scattering (RIXS), that the values of effective spin-orbit coupling ($\lambda \sim 0.39$ eV) and Hund's exchange ($J_H \sim 0.25$ eV) for Ba_2YIrO_6 are comparable. Although RIXS shows $J \neq 0$ states to be largely separated (> 0.37 eV) from the $J = 0$ non-magnetic spin state, hopping among Ir-Ir sites not only reduces the effect of SOC but also spontaneously generates tiny moments due to inter-mixing of the J states. Interestingly, from Muon Spin Relaxation (μSR) we find these tiny moments to fluctuate slowly down to 60 mK pointing towards a resonating valence bond state.

In recent years, $5d$ transition metal oxides which were predicted to be weakly correlated wide band metals, have surprisingly shown the presence of Mott-insulating states with unusual electronic and magnetic properties, owing to strong spin-orbit coupling (SOC) comparable to bandwidth W [1, 2]. It has been observed that in tetravalent iridates (Ir^{4+} ; $5d^5$), SOC (λ) splits t_{2g} orbitals into fully filled $j_{\text{eff}} = \frac{3}{2}$ quartet and half filled narrow $j_{\text{eff}} = \frac{1}{2}$ doublet, which under a small Hubbard U further splits into fully occupied lower and empty upper Hubbard bands, creating the Mott state [3].

An interesting deviation from such a situation arises in pentavalent iridates (Ir^{5+} ; $5d^4$) within the strong spin-orbit coupled multiplet scenario, where one may end up with a non-magnetic $J = 0$ ($M_J = 0$) ground state [4]. Strong crystal field splitting (Δ_{CFE}) underscores Hund's exchange energy (J_H) in the $5d$ levels, leading to a low spin $S = 1$ for t_{2g}^4 electrons in such Ir^{5+} ions in the absence of SOC. The projection of orbital angular momentum onto the degenerate t_{2g} orbitals, gives an effective orbital angular momentum $L_{\text{eff}} = -1$ that couples with S , producing ${}^6C_4 = 15$ (4 electrons in 6 spin-polarized degenerate t_{2g} orbitals) possible arrangements/ J states. Effects of SOC (λ) in such situations however, can only be conceived comprehensively within multiplet picture which modifies stability of various spin-orbit coupled (LS/jj) multiplet states depending upon the strength of λ (Fig. 1(a)) [5]. In a solid in the presence of hopping the SOC may be comparable to superexchange energy scales $4t^2/U$ inducing Van-Vleck singlet-triplet excitonic magnetism [5, 6]. Moreover, in solids or clusters, crystal field effects (Δ_{CFE}), non-cubic distortions of the atomic octahedra further modify the energy separation of the multiplet states, effectively changing the λ severely [7–9]. As a result, no $5d^4$ system possessing strong enough SOC, showing an absolutely non-magnetic $J = 0$ state has been realized so far [5, 8, 10–12]. In other words, solid state and crystal field effects always drive these systems towards a magnetic $J \neq 0$ state.

Interestingly, all these systems are found to be electrically insulating, indicating presence of clear band gaps in the charge sector [5, 8, 10–12], as often is the case for Van-Vleck systems. Here also, the driving factor is SOC, which induces an insulating state in d^4 systems. In fact, often these spontaneous moments are antiferromagnetically coupled in a frustrated lattice giving rise to quantum spin orbital liquid state [5], a highly correlated strongly fluctuating spin state without broken symmetries as $T \rightarrow 0$ K, or a weakly resonating valence bond state or even a static gapped valence bond solid [13, 14]. SOC together with frustration can therefore tune the system from a gapless spin-liquid state to a gapped non-magnetic state

to generate a rich phase diagram.

A suitable choice to study single ion properties with minimal solid state and non-cubic crystal field effects can be a double perovskite like Ba_2YIrO_6 . Here, in an ordered arrangement of Ir^{5+} ions separated by non-magnetic Y^{3+} , a $J = 0$ ground state may be stabilized. Also, its $Fm\bar{3}m$ space group does not allow any IrO_6 octahedral distortion thereby maximizing the effects of SOC [8, 15]. Only hopping can then compete against SOC to generate magnetic moments in Ba_2YIrO_6 [16]. Recent investigations on the ground state properties of this system however, has been flooded with conflicting results. While one group, from first principles calculations found dominant antiferromagnetic exchanges and large Ir bandwidth breaking down the $J = 0$ state [17], another group questions the idea of ordered magnetism due to stabilisation of a non-magnetic state [18]. On the other hand among experimentalists, Zhang *et. al.* reported a large magnetic moment of $1.44 \mu_B/\text{Ir}$ with antiferromagnetic ordering at ~ 1.5 K [19], whereas T. Dey *et. al.* found correlated magnetic moments ($0.44 \mu_B/\text{Ir}$) that do not order till 0.4 K, contrary to their theoretical calculations [11].

In this paper, we calculate the value of λ and J_H from Resonant Inelastic X-Ray Scattering (RIXS) on Ba_2YIrO_6 , and find that despite having perfectly cubic crystal field and isolated Ir^{5+} ions, effective λ is only ~ 0.39 eV, comparable to other Ir oxide double perovskites with distortions [20]. While the RIXS excitation spectra could be fitted with an effective atomic model, the presence of the magnetic moments suggest that the ground state is not a pure $J = 0$ state, due to hopping induced mixing among the states. Interestingly, these moments are coupled by antiferromagnetic exchange interaction on a frustrated FCC lattice and tend to form spin singlets. We find from Muon Spin Relaxation (μSR) that these moments fluctuate slowly down to at least 60 mK forming a resonating valence bond kind of state [7, 14].

Polycrystalline Ba_2YIrO_6 was synthesized by standard solid state reaction using stoichiometric amounts of BaCO_3 , Y_2O_3 and Ir-metal as starting materials [15]. The sample purity was checked and refined by powder X-Ray diffraction measured in the Indian beamline (BL-18B) at Photon Factory, KEK, Japan and MCX beamline, Elettra (Trieste, Italy). Neutron powder diffraction (NPD) patterns were recorded at wavelength 1.48\AA in National Facility for Neutron Beam Research (NFNBR), Dhruva reactor, Mumbai (India). The data were refined using Rietveld method using FULLPROF [21]. The X-ray photoelectron spectroscopic (XPS) measurements were carried out in a lab based Omicron electron spectrometer,

TABLE I. Main structural parameters obtained from the Multi-shell fitting of the Ir L_3 -edge EXAFS spectra. The crystallographic distances, as obtained by NPD Rietveld refinement at 300 K, are reported for sake of comparison.

Shell	N	$R_{\text{EXAFS}}(\text{\AA})$	$\sigma^2(\times 10^{-3} \text{\AA}^2)$	$R_{\text{NPD}}(\text{\AA})$
Ir-O	6	1.979(5)	3.2(2)	1.968(4)
Ir-Ba	8	3.62(1)	7.9(5)	3.62(8)
Ir-Y	6	4.17(1)	19(1)	4.17(6)

equipped with EA125 analyzer. The electrical resistivity measurements were done in four probe configuration in a lab based experimental set up. The dc magnetic measurements and heat capacity measurements were carried out using a Quantum Design SQUID magnetometer and a Quantum Design PPMS (physical property measurement system) at Materials and Structural Laboratory, Tokyo Institute of Technology respectively. X-Ray Absorption spectra at the Ir L_3 -edges were collected at the Elettra (Trieste, Italy) 11.1R-EXAFS beamline in standard transmission geometry at room temperature. μ SR experiments were performed with the EMU spectrometer at the ISIS large scale facility both in a helium flow cryostat and a dilution fridge. Resonant Inelastic X-ray Scattering was done at ESRF ID20 (C11) under the proposal ID HC-2872 on polycrystalline sample at 20 K.

Neutron Powder Diffraction data recorded on Ba_2YIrO_6 at 300 K and 2.8 K (Fig. 1(b)) show that no structural transition is present down to 2.8 K; except for a lattice contraction. The Y/Ir ordered $Fm\bar{3}m$ structure obtained from refinement is depicted in Fig. 1(c). The powder diffraction results match well with earlier reports [15]. The atomic positions are: Ba (1/4, 1/4, 1/4), Y (0, 0, 0), Ir (1/2, 1/2, 1/2), and O (x , 0, 0). For Neutron diffraction at 300 K and 2.8 K, $x = 0.2644(4)$ and $0.2647(4)$; and $a = 8.352$, and 8.3422 respectively. $\chi^2_{300K} = 3.36$ and $\chi^2_{2.8K} = 3.44$. This space group ensures a regular IrO_6 octahedra with cubic crystal field on Ir ions. Local structure obtained by EXAFS at Ir L_3 edge as shown in Fig. 2 and presented in Table I, confirms negligible Y/Ir site disorder ($< 1\%$). We used a multi-shell data fitting to get chemical order information from next neighbour coordination shell analysis according to our previous analysis [22]. Unlike single crystal samples, Hammerath *et. al.* too, recently reported polycrystals to be devoid of Y_2O_3 impurities and much lower antisite disorder ($< 1.5\%$) [23].

X-ray photoelectron spectroscopy confirms the presence of Ir^{5+} ions only. The XPS spectra for the Ir $4f$ core level could be fitted by spin-orbit split doublet of $4f_{5/2}$ and $4f_{3/2}$ with a separation of 3.01 eV (Fig. 3(a)). The energy position of the doublet confirms +5 oxidation or d^4 electronic state of Ir [24]. The electronic nature of Ba_2YIrO_6 was found to be insulating and the resistivity (ρ) could be modeled by Mott variable range hopping mechanism in 3-dimensions (Fig. 3(b)). The gapped nature was further tested by measurement of valence band photoemission experiment, where absence of any density of states at the Fermi level (Fig. 3(c)) was confirmed. Our observation of low density of states at the Fermi level in valence band photoemission spectrum and insulating nature of the material immediately suggests the importance of SOC, without which a $5d^4$ state should have been metallic (Fig. 1(a)).

In spite of strong SOC, the dc magnetic susceptibility measured in 3 T field (Fig. 1(d)) shows presence of tiny magnetic moments which do not order down to 2 K, having qualitative similarity to paramagnets. The χ vs. T curves are fitted with $\chi_0 + C_W/(T - \theta_W)$ for different temperature ranges where χ_0 is the temperature independent susceptibility, C_W and θ_W represent Curie constant and Curie-Weiss temperature, respectively. One can observe a gradual increase in the magnetic moments as one goes towards higher temperature ranges of fitting (Fig. 4), however, the extracted moment remains close to a value of $\sim 0.3 \mu_B/\text{Ir}$ for all ranges [25]. Antiferromagnetic interaction ($\theta_W = -10$ K) is also evident from the CW fitting for the different fitting temperature ranges. This value of magnetic moment is identical to that reported by Hammerath *et. al.* recently, on polycrystalline sample of Ba_2YIrO_6 [23]. With a larger number of defects, the single crystals have always shown larger magnetic moment values [11, 19, 26]. Hammerath *et. al.* propose the moments to originate from 2-5% $\text{Ir}^{4+}\text{Ir}^{6+}$ ions, while the rest of the ions form a non-magnetic $J = 0$ background but this description does not account for the antiferromagnetic correlations observed experimentally. In the strong SOC regime, the $J = 0$ insulating state is expected to be stabilized even without invoking the correlation effects. However, theoretical calculations are not found to reproduce the experimentally observed insulating state in presence of SOC without including correlations [11, 18]. Chen *et. al.*'s recent report on the other hand describes the moments to arise due to enhanced exchanges because of (Y/Ir) disorder [26]. To explain a moment of $0.3 \mu_B/\text{Ir}$, according to their description one needs a disorder of at least 3% that is neither found by us from EXAFS ($< 1\%$) nor by Hammerath *et. al.* from

Nuclear Magnetic Resonance (NMR) experiments ($< 1.5\%$). One should note that each one of the disorder creates 6 new Ir-O-Ir pairing, thus 3% disorder and the resulting 6 times larger Ir-O-Ir network would be easily tracked through EXAFS. Also, this estimate assumes that all these spins are excited to $J = 1$ state, which is the upper bound of excitation [26]. Then if we consider these moments to contribute to Van-Vleck magnetism, the origin of the Curie contribution antiferromagnetic correlations remains unaccounted for. Thus, while disorder will lead to enhancement in superexchange interactions sufficient for singlet-triplet excitation, it alone cannot explain the magnetic moments observed.

Unlike for d^5 systems where J_H does not have any effect on the separation of the multiplets, for d^4 systems it is the competition between the λ and J_H that determines the extent of separation between the J states [16]. One therefore needs to find out the positions of the higher excited non-magnetic states and evaluate both λ and J_H , to understand the origin of these magnetic moments. We did RIXS measurement at the Ir L_3 edge of Ba_2YIrO_6 and $T = 20$ K with the incident photon energy fixed at 11.216 keV, that was found to enhance the inelastic features of the J multiplet excitations. Increased photon counts at particular energy losses in the RIXS spectrum (Fig. 5(a)) represent specific excitations from filled to vacant electronic states. For example, the largest energy loss features (~ 5.73 and ~ 8.67 eV) can be ascribed to charge transfer excitations from the O $2p$ bands to vacant Ir energy bands [27]. The feature observed at ~ 3.61 eV is due to the electron excitation from t_{2g} to e_g orbitals representing the crystal-field excitations. Our single particle mean-field calculations using muffin-tin orbital (MTO) based N^{th} order MTO (NMTO) method as implemented in Stuttgart code [28] showed Δ_{CFE} to be 3.45 eV, close to the experimental value showing its effectiveness in estimating the gap to the SOC unaffected e_g levels. We observe three sharp inelastic peaks in the highly resolved RIXS spectrum below 1.5 eV (Fig. 5(a)) which are significantly different from the peaks seen in Ir^{4+} systems [29]. This difference arises because while for Ir^{4+} , excitations occur within the $j_{\text{eff}} = \frac{3}{2} \rightarrow \frac{1}{2}$ manifold [3], here the multiplet states are $J = 0, 1, 2$ and so on (Fig. 1(a)). The low energy peaks were fitted with Lorentzian functions giving energy losses at 0.35, 0.60 and 1.18 eV. Fig. 5(a) shows these energy losses as vertical bands having widths given by the experimentally obtained FWHMs 0.033(4), 0.048(3) and 0.10(1) eV respectively. In order to extract λ and J_H , these energy losses were mapped with the energy differences between the states obtained from effective

full many-body atomic Hamiltonian

$$H_{atomic} = H^{int} + H^{SO}, \quad (1)$$

where, H^{int} and H^{SO} are the Hamiltonian for the Coulomb interaction and the SOC on the three t_{2g} orbitals respectively [5, 20, 30, 31]. The t_{2g} orbitals are well separated from the e_g orbitals due to the strong octahedral crystal field in the pentavalent iridate Ba_2YIrO_6 . Further the d^4 electronic configuration makes the t_{2g} orbitals to be the only active orbitals while we can safely ignore the e_g orbitals which is however not the case for $3d$ TMOs. Now, the interaction part of the Hamiltonian in Eqn. 1 has the Kanamori form [30, 31],

$$\begin{aligned} H^{int} = & U_d \sum_{l=1,2,3} n_{l\uparrow} n_{l\downarrow} + \frac{U'_d - J_H}{2} \sum_{\substack{l,m=1,2,3 \\ (l \neq m)}} \sum_{\sigma} n_{l\sigma} n_{m\sigma} + \frac{U'_d}{2} \sum_{\sigma \neq \sigma'} \sum_{\substack{l,m=1,2,3 \\ (l \neq m)}} n_{l\sigma} n_{m\sigma'} \\ & + \frac{J_H}{2} \sum_{\substack{l,m=1,2,3 \\ (l \neq m)}} (d_{l\uparrow}^\dagger d_{m\uparrow} d_{l\downarrow}^\dagger d_{m\downarrow} + h.c.) \end{aligned} \quad (2)$$

where, U_d , U'_d and J_H are respectively intra-Coulomb interaction, inter-Coulomb interaction and Hund's rule coupling and they are related as $U_d = U'_d + 2J_H$. $d_{l\sigma}(d_{l\sigma}^\dagger)$ is the annihilation (creation) operator of the l^{th} orbital ($l = 1, 2, 3$) with a spin σ and $n_{l,\sigma} = d_{l,\sigma}^\dagger d_{l,\sigma}$. The explicit form of spin-orbit interaction is given by [31],

$$H^{SO} = \frac{i\lambda}{2} \sum_{lmn} \epsilon_{lmn} \sum_{\sigma\sigma'} \sigma_{\sigma\sigma'}^n d_{l\sigma}^\dagger d_{m\sigma'} \quad (3)$$

where, λ is the magnitude of spin-orbit interaction between orbital (l_i) and spin (s_i) angular momenta of the i^{th} electron and ϵ_{lmn} is the Levi-Civita symbol.

Owing to the perfect cubic symmetry of Ba_2YIrO_6 , the t_{2g} levels are completely degenerate and hence no non-cubic crystal field is taken into account. The Hamiltonian in Eqn. 1, is diagonalised in the Hilbert space spanned by ${}^6C_4 = 15$ (four electrons are arranged among the six-fold degenerate t_{2g} states considering the spin degeneracy) basis states. Exact diagonalisation of this atomic model Hamiltonian gives the energy eigen values of the ground state and the subsequent excited states. The energy differences of these states, which is independent of U_d , can be directly mapped to the peak positions obtained in RIXS probing the low energy elementary excitations in condensed matter systems.

As shown in Fig. 5(b), the calculated energy differences simultaneously match with the three corresponding experimental energy loss bands giving $\lambda = 0.39$ eV, for a range of $J_H = 0.24$ - 0.26 eV. The value of the SOC obtained by fitting the RIXS data places Ba_2YIrO_6 in the intermediate SOC regime. An exact diagonalisation calculation with two-site model with our estimated values of λ and J_H , in addition allowing hopping between the two sites not only produces spontaneous magnetic moment but also favor singlet state with antiferromagnetic alignment between the moments [16]. One should note that assuming the singlet-triplet excitation gap to be equivalent to the first energy loss position (~ 0.37 eV) in the RIXS spectra, by considering an atomic model description and comparing it with the small superexchange energies in completely ordered material is not strictly correct. This is because, as soon as one introduces hopping in the model, even if they are small, the very nature of the lowest energy state changes from $J = 0$, thereby giving rise to non-zero total angular momentum to the ground state at each Ir site as can be noted from Svoboda *et al.*'s work [16]. Thus it is more likely that magnetic moments are generated in all Ir ions due to hopping but the hopping itself is so small that its signature is invisible to RIXS. A full cluster calculation taking into account hopping between the 12 neighbouring Ir sites, may therefore be able to capture the essential physics and a proper estimate of the spin-excitation gap.

In compounds such as Ba_2YIrO_6 where both single ion properties and lattice frustration combine to prohibit classical Néel order, signatures of a possible complex magnetic ground state can be elusive and hardly detectable in macroscopic measurements. In order to investigate accurately the nature of magnetism, we further used the μSR technique which is uniquely sensitive to tiny internal fields. The measured time-evolution of the muon polarization $P(t)$ in zero external field is shown in Fig. 6(a) for some selected temperatures. Down to base temperature 60 mK, we observed no signature of static magnetism, neither long range ordered nor disordered. At all temperatures, the polarization could be fitted to a stretched exponential $P(t) = e^{-(\lambda' t)^\beta}$. The temperature variation of the fitting parameters λ' and β is shown in Fig. 6(b). On cooling down, we observe a rather weak and gradual increase of the relaxation, corresponding to a slowing down of the spin dynamics since $\lambda' \propto 1/\nu$, where ν is the characteristics spin fluctuation frequency, which levels off below 1 K showing persistent spin fluctuations down to 60 mK. There is no signature of magnetic freezing such as fast relaxation, loss of initial asymmetry or apparition of a finite long time limit $P(t \rightarrow \infty)$. To

get more insight into the origin of the relaxation observed at low temperature, we investigated the evolution of the polarization at 1.6 K, at the onset of the relaxation plateau, with an external longitudinal field B_{LF} . As can be seen in Fig. 6(c), weak applied fields of a few mT reduce the relaxation quite strongly, showing that the internal fields B_μ probed by the muons are extremely weak and fluctuate very slowly. A crude estimate of B_μ and ν from Redfield formula $\lambda' = \nu\gamma_\mu^2 B_\mu^2 / (\nu^2 + \gamma_\mu^2 B_{LF}^2)$ (see inset to Fig. 6(c)) yields $B_\mu \sim 0.2$ mT and $\nu \sim 1.2$ MHz. Assuming that the positively charged muons stop close to the negative oxygen ions in the structure, *i. e.* about 2 Å away from the Ir ions, the fluctuating moments needed to produce the dipolar field B_μ , are as low as $10^{-3} \mu_B$. It is therefore more realistic to consider that the small internal fields observed by the muons arise from diluted magnetic centers out of a non-magnetic background. From the value of B_μ , we estimate the concentration of $0.3 \mu_B$ Ir moments to be as small as ~ 0.002 [32]. This is supported by the observation of the change in β as shown in the lower panel of Fig. 6(b) from ~ 0.8 at high temperatures to ~ 0.55 below 1 K, reflecting the emergence of an inhomogeneous magnetic environment for the muons at low temperature [32]. Similar to our observation from μ SR, Dey *et. al.* too, recently find a non-magnetic background with isolated spins from NMR. While they describe it in terms of a non-magnetic background of $J = 0$ state interspersed with impurity paramagnetic spins, this does not explain the presence of antiferromagnetic correlations observed from other experiments [11, 23]. Moreover, our estimation of these isolated spins of $0.3 \mu_B$ Ir moments are as small as ~ 0.002 from μ SR, which cannot alone account for the magnetic susceptibility. A possibility therefore can be, that most of the $0.3 \mu_B$ Ir moments pair up to form a weakly resonating valence bond state of slowly fluctuating singlets with vanishing magnetisation at low T (See Fig. 6(b)) and a few unpaired Ir ions are left out (due to Y/Ir disorder below our sensitivity to structural disorder (EXAFS, NPD), with a very low residual interaction between them. This is similar to the scenario proposed for Ba_2YMoO_6 [13], and shows the strength of μ SR to discern infinitesimal amounts of isolated magnetic ions which are often a cause for non-saturating bulk magnetic susceptibility in frustrated systems [33–35].

To further probe the low energy magnetic states, heat capacity (C) of Ba_2YIrO_6 was measured. C vs T (Fig. 7(a)) shows a broad hump around 5 K, however, absence of a sharp anomaly indicates absence of a thermodynamic phase transition into long range antiferromagnetic order of these small moments, which is also supported by the absence of magnetic

peaks or diffuse background in NPD of 2.8 K (Inset to Fig. 7(c)). The magnetic heat capacity (C_m) was extracted by subtracting the lattice contribution using isostructural non-magnetic Ba_2YSbO_6 and Bouvier scaling procedure [36]. The obtained C_m is plotted in Fig. 7(b), which shows a linear decay below 5 K pointing towards slowing down of spin dynamics. A low temperature fit of the magnetic heat capacity gives a large T -linear component of ~ 176 mJ/mol-K², unusual for charge insulators. This may be an indirect evidence of intrinsic gapless spin excitations similar to reported gapless quantum spin liquids or presence of spinon Fermi surface [13, 14, 37–39]. The C also does not show any variation up to applied fields of 9 T, showing its origin to be from intrinsic excitations and not any paramagnetic defects (Fig. 7(c)) [37, 40].

On cooling to a completely ordered state, the total magnetic entropy loss of the system in a multiplet scenario would be equal to $R\ln(2J+1)$ where J is the spin state accessed by the electrons. For Ba_2YIrO_6 , the total magnetic entropy S_m released, obtained by integrating C_m/T with T as shown in Fig. 7(d) has only a value of ~ 1.03 J/mol-K-Ir (~ 11 %) till 25 K. This large residual entropy should be the outcome of a highly degenerate ground state of resonating Ir-Ir non-magnetic singlets [14, 41].

In conclusion, we find that the ground state of Ba_2YIrO_6 is a slowly resonating valence bond state promoted by SOC. However, from RIXS we find that the SOC is not strong and the system lies in the intermediate SOC regime (Arrow in Fig. 1(a)). Hopping induced superexchange is so minute that it produces tiny moments but is untraceable by RIXS. μSR shows presence of weakly correlated moments in trace amounts on an overall non-magnetic background probably formed by slowly fluctuating singlets down to 60 mK. A material with an even stronger λ is therefore required for the observation of a true non-magnetic $J = 0$ ground state, although solid state effects like hopping always will act against and favor generation of magnetic moments.

A.N. and S. B. thank Indian Association for the Cultivation of Science, and Council of Scientific & Industrial Research (CSIR), India respectively for fellowship. S. R. thanks Department of Science and Technology (DST) [Project No. WTI/2K15/74] for funding, and for financial support by Indo-Italian Program of Cooperation, Saha Institute of Nuclear Physics, Collaborative Research Projects of Materials and Structures Laboratory at Tokyo Institute of Technology (TiTech), Newton-India fund, Jawaharlal Nehru Centre for Advanced Scientific Research from DST-Synchrotron-Neutron project, for performing ex-

periments at Elettra (Proposal No. 20140355), Photon Factory, TiTech, ISIS, and ESRF respectively F. B. thanks financial support from project SOCRATE (ANR-15-CE30-0009-01) of French National Research Agency. S. R. and I. D. thank TRC, Department of Science and Technology (DST), Government of India for support.

* Email:mssr@iacs.res.in

- [1] W. Witczak-Krempa, G. Chen, Y. B. Kim, and L. Balents, *Annu. Rev. Condens. Matter Phys.* **5**, 57 (2014).
- [2] J. G. Rau, E. K.-H. Lee, H.-Y. Kee, *Annu. Rev. Condens. Matter Phys.* **7**, 195 (2016).
- [3] B. J. Kim *et. al.*, *Phys. Rev. Lett.* **101**, 076402 (2008).
- [4] J. Rublo, and J. J. Perez, *J. Chem. Education* **63**, 476 (1986).
- [5] A. Nag *et. al.*, *Phys. Rev. Lett.* **116**, 097205 (2016).
- [6] G. Khaliullin, *Phys. Rev. Lett.* **111**, 197201 (2013).
- [7] G. Chen, L. Balents, and A. P. Schnyder, *Phys. Rev. Lett.* **102**, 096406 (2009).
- [8] G. Cao, T. F. Qi, L. Li, J. Terzic, S. J. Yuan, L. E. DeLong, G. Murthy, and R. K. Kaul, *Phys. Rev. Lett.* **112**, 056402 (2014).
- [9] T. Dodds, T. P. Choy, and Y. B. Kim, *Phys. Rev. B* **84**, 104439 (2011).
- [10] M. A. Laguna-Marco, P. Kayser, J. A. Alonso, M. J. Martinez-Lope, M. van Veenendaal, Y. Choi, and D. Haskel, *Phys. Rev. B* **91**, 214433 (2015).
- [11] T. Dey, *et. al.*, *Phys. Rev. B* **93**, 014434 (2016).
- [12] M. Bremholm, S. E. Dutton, P. W. Stephens, and R. J. Cava, *J. Solid State Chem.* **184**, 601 (2011).
- [13] M. A. de Vries, A. C. Mclaughlin, and J.-W. G. Bos, *Phys. Rev. Lett.* **104**, 177202 (2010).
- [14] L. Balents, *Nature* **464**, 199 (2010).
- [15] W. T. Fu, and D.J.W. IJdo, *J. Alloys Compd.* **394**, L5 (2005).
- [16] C. Svoboda, M. Randeria, and N. Trivedi, *Phys. Rev. B* **95**, 014409 (2017).
- [17] S. Bhowal, S. Baidya, I. Dasgupta, and T. S.-Dasgupta, *Phys. Rev. B* **92**, 21113(R) (2015).
- [18] K. Pajskr, P. Novák, V. Pokorný, J. Kolorenč, R. Arita, and J. Kuneš, *Phys. Rev. B* **93**, 035129 (2016).
- [19] H. Zhang, J. Terizc, F. Ye, P. Schlottmann, H. D. Zhao, S. J. Yuan, and G. Cao, *arXiv:1608.07624* (2016).
- [20] B. Yuan, *et. al.*, *Phys. Rev. B* **95**, 235114 (2017).
- [21] J. Rodríguez-Carvajal, *Physica B* **192**, 55 (1993).
- [22] C. Meneghini, Sugata Ray, F. Liscio, F. Bardelli, S. Mobilio, and D. D. Sarma, *Phys. Rev.*

- Lett. **103**, 046403 (2009).
- [23] F. Hammerath *et. al.*, arXiv:1707.06027 (2017).
 - [24] T. Otsubo, S. Takase, and Y. Shimizu, ECS Transactions **3** (1), 263 (2006).
 - [25] A. Nag, and S. Ray, J. Magn. Magn. Mater. **424**, 93 (2017).
 - [26] Q. Chen *et. al.*, arXiv:1707.06980 (2017).
 - [27] K. Ishii, I. Jarrige, M. Yoshida, K. Ikeuchi, J. Mizuki, K. Ohashi, T. Takayama, J. Matsuno, and H. Takagi, Phys. Rev. B **83**, 115121 (2011).
 - [28] O. K. Andersen and T. Saha-Dasgupta, Phys. Rev. B **62**, 16219(R) (2000); O. K. Andersen, T. Saha-Dasgupta, R. W. Tank, C. Arcangeli, O. Jepsen, and G. Krier, Electronic Structure and Physical Properties of Solids. The Uses of the LMTO Method, Springer Lecture Notes in Physics (Berlin: Springer), **3** (2000); O. K. Andersen, T. Saha-Dasgupta, and S. Ezhov, Bull. Mater. Sci. **26**, 19 (2003).
 - [29] M. Moretti Sala, K. Ohgushi, A. Al-Zein, Y. Hirata, G. Monaco, and M. Krisch, Phys. Rev. Lett. **112**, 176402 (2014).
 - [30] J. Kanamori, Prog. Theor. Phys. **30**, 275 (1963).
 - [31] H. Matsuura and K. Miyake, J. Phys. Soc. of Jpn. **82**, 073703 (2013).
 - [32] Y. J. Uemura, T. Yamazaki, D. R. Harshman, M. Senba, and E. J. Ansaldo, Phys. Rev. B **31**, 546 (1985).
 - [33] A. Olariu, P. Mendels, F. Bert, F. Duc, J. C. Trombe, M. A. de Vries, and A. Harrison, Phys. Rev. Lett. **100**, 087202 (2008).
 - [34] R. R. P. Singh, Phys. Rev. Lett. **104**, 177203 (2010).
 - [35] M. Gomilsek, M. Klanjsek, M. Pregelj, H. Luetkens, Y. Li, Q. M. Zhang, and A. Zorko, Phys. Rev. B **94**, 024438 (2016).
 - [36] M. Bouvier, P. Lethuillier, and D. Schmitt, Phys. Rev. B **43**, 13137 (1990).
 - [37] L. Clark *et. al.*, Phys. Rev. Lett. **110**, 207208 (2013).
 - [38] M. R. Norman, and T. Micklitz, Phys. Rev. Lett. **102**, 067204 (2009).
 - [39] Y. Shen, *et. al.*, Nature **540**, 559 (2016).
 - [40] S. Yamashita, Y. Nakazawa, M. Oguni, Y. Oshima, H. Nojiri, Y. Shimizu, K. Miyagawa, and K. Kanoda, Nat. Phys. **4**, 459 (2008).
 - [41] A. P. Ramirez, B. Hessen, and M. Winklemann, Phys. Rev. Lett. **84**, 2957 (2000).
 - [42] K. Momma, and F. Izumi, J. Appl. Crystallogr. **44**, 1272 (2011).

- [43] B. Koteswararao, *et. al.*, Phys. Rev. B **90**, 035141 (2015).
- [44] Y. Okamoto, M. Nohara, H. Aruga-Katori, and H. Takagi, Phys. Rev. Lett. **99**, 137207 (2007).

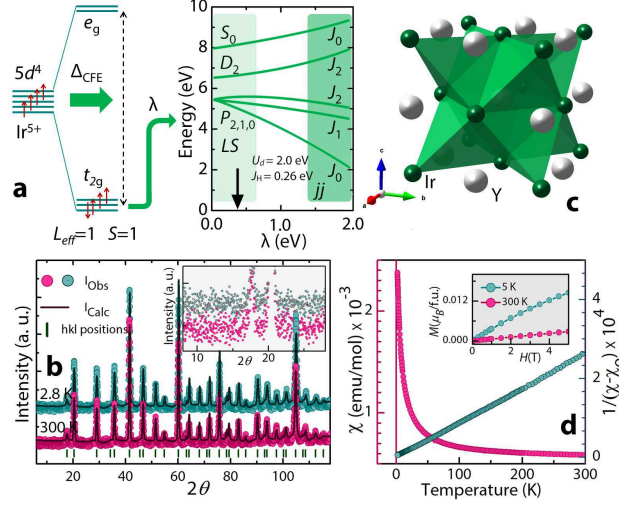


FIG. 1. (a) Reorganisation of d^4 orbitals under octahedral crystal field and then SOC to form multiplet spin-orbit coupled states [5]. (b) Experimental and refined neutron powder diffraction patterns with Bragg reflections. Inset shows enlarged low angle background of the two patterns. (c) Edge shared tetrahedral network of Ir atoms on a FCC lattice in cubic Ba_2YIrO_6 [42]. (d) Magnetic susceptibility χ vs. T and $1/(\chi-\chi_0)$ vs. T measured with 3 T field is shown. An inset shows the $M(H)$ isotherms at 5 K and 300 K.

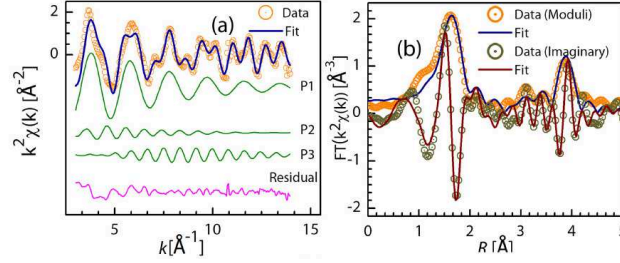


FIG. 2. (a) The k^2 weighted XAFS data from Ir L_3 edge of BYIO and best fit and residual are presented. The partial contributions from different scattering paths are shown: Path1: Ir-O, Path2: Ir-Ba, The path P3 includes single (Ir-O-Ir) and multiple (Ir-O-Y-Ir and Ir-O-Y-O-Ir) scattering terms corresponding to the aligned Ir-O-Y configurations. (b) The moduli and imaginary parts of Fourier transforms of k^2 weighted XAFS data and best fit data.

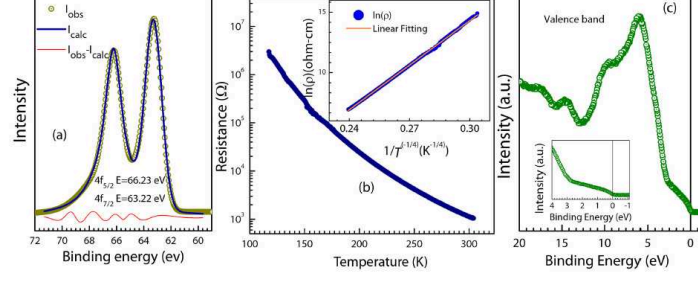


FIG. 3. (a) XPS spectra for the Ir 4f core level fitted by spin-orbit split doublet, (b) Four probe resistivity of BYIO fitted with VRH model (inset) and (c) XPS spectra for the valence band of BYIO, recorded with Mg K_{α} radiation.

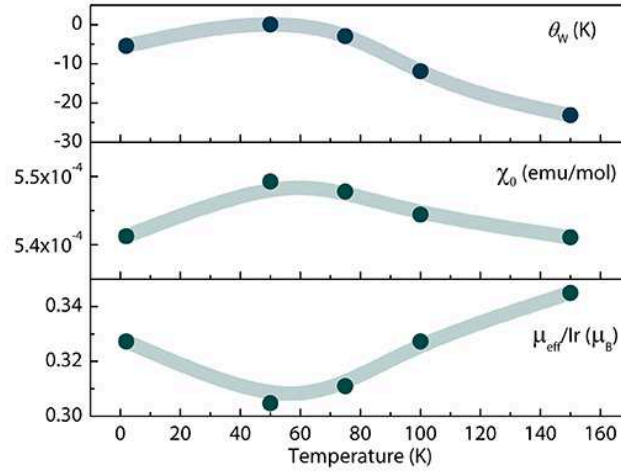


FIG. 4. Fitting parameters (θ_W , χ_0 and $\mu_{\text{eff}}/\text{Ir}$) extracted from CW fitting of 3 T ZFC χ as a function of fitting range (T -300 K)

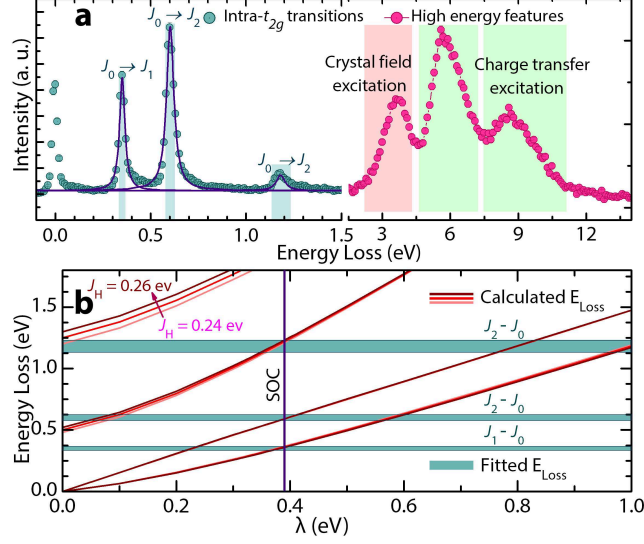


FIG. 5. (a) RIXS spectrum of Ba_2YIrO_6 with the left hand side showing the high resolution low energy excitations within the SOC multiplets and the high energy features shown to the right. Individual peak fits are shown by continuous lines. Experimentally obtained energy losses with their corresponding FWHMs are shown as vertical bands in (a) and horizontal bands in (b). Calculated energy differences between the SOC multiplets for three different J_H (0.24-0.26 eV), according to Eq. 1 are shown, that intersect simultaneously the horizontal bands for $\lambda = 0.39$ eV.

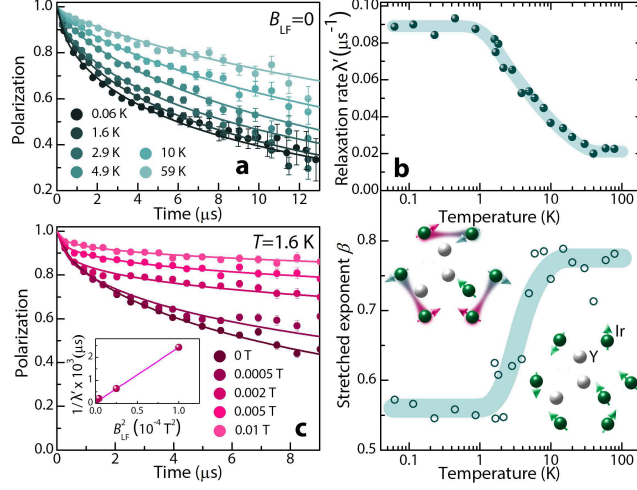


FIG. 6. (a) Time evolution of the muon polarization in Ba_2YIrO_6 in zero field with fits to a stretched exponential (continuous lines). (b) Fitting parameters λ' (upper panel) and β (lower panel) extracted from the fits (see text). While at higher temperatures all spins behave identically giving a uniform magnetic distribution, below ~ 10 K a non-magnetic background of Ir-Ir singlets is observed interspersed by minute amounts of isolated Ir spins due to (Y/Ir) disorder, as depicted schematically in the lower panel. (c) Evolution of the muon polarization with an applied longitudinal field at 1.6 K. Inset : relaxation times ($1/\lambda'$) obtained from the fits of the polarizations (lines in the main panel) as a function of the square of the longitudinal applied field B_{LF} .

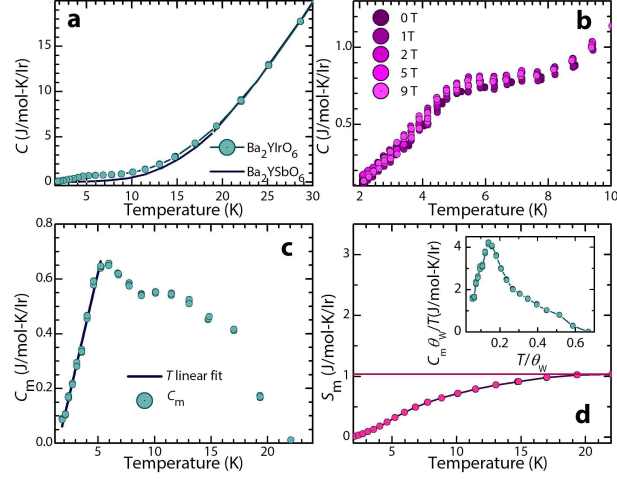


FIG. 7. Temperature dependence of (a) specific heat (C) of Ba_2YIrO_6 and Ba_2YSbO_6 and (b) the effect of external magnetic fields on the feature ~ 5 K. (c) Magnetic heat (C_m) capacity obtained after subtracting the lattice contribution along with linear fit. (d) Magnetic entropy S_m released obtained by integrating C_m/T . Inset: C_m peaking around $T/\theta_W \sim 0.14$ like in other frustrated systems [43, 44].